

Supporting Information

POM-based Metal Organic Frameworks with Woven Fabric Structure for Lithium Storage

Meng-Ting Li,^{a,b*}Jing-Wen Sun,^c Yi-Fei-Liu,^a Mei-Hui Niu,^a Han-Yu Zou,^a Da-Qiang Sun,^{*b} and Yang Yu^{*a}

a School of Chemistry and Chemical Engineering, Qufu Normal University, Qufu 273165, Shandong, China

b Shandong Sacred Sun Power Sources Co., Ltd. No.1, Shengyang Road, Qufu, Shandong 273100, China

c School of Pharmacy, Qiqihar Medical University, Qiqihar 161006, Heilongjiang, China

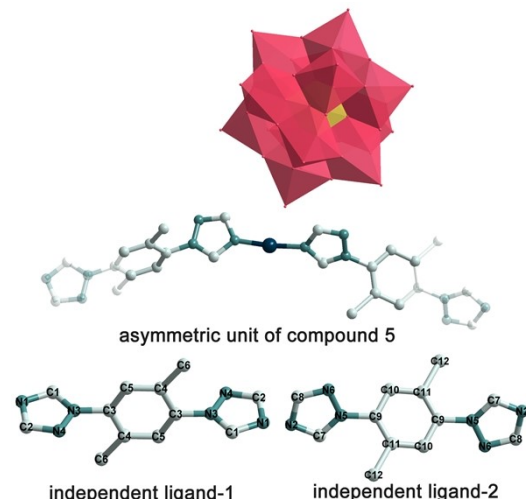


Figure S1 Ball/stick/polyhedral view of the crystallographic unit and the ligands coordination pattern of Cu-BTDB-POM. All of the hydrogen atoms were omitted for clarity.

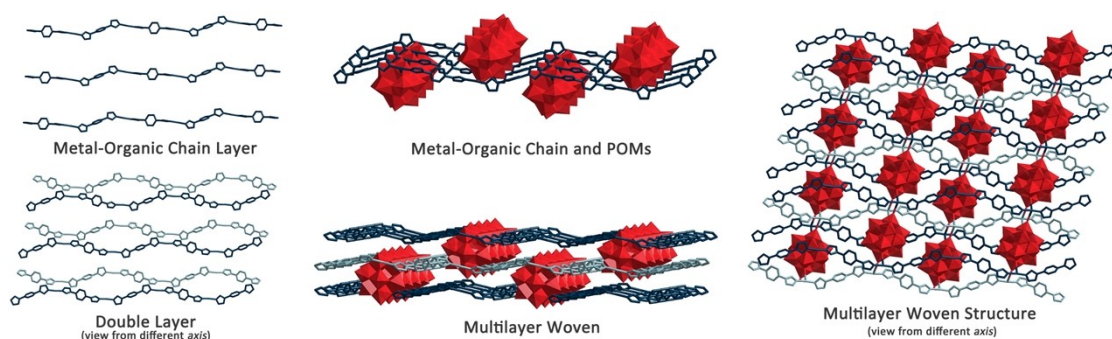


Figure S2 Ball/stick/polyhedral view of the metal-organic chain layer and the woven structure of Cu-BTDB-POM. The woven structure is composed of metal-organic chain and POMs metal-inorganic chain. All of the hydrogen atoms were omitted for clarity.

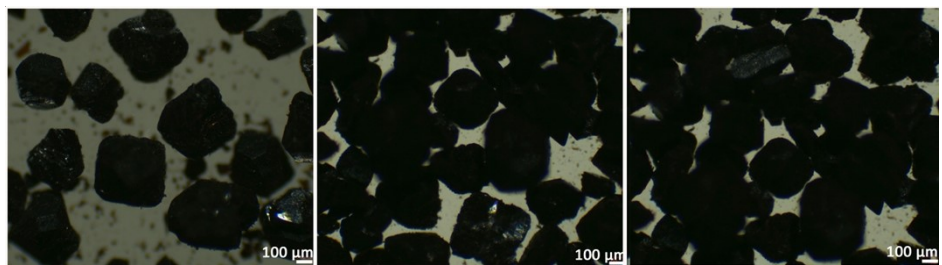


Figure S3 Light microscope photograph of the crystalline Cu-BTDB-POM. The maximum crystal size is about 600 μm , and the average size is 350~400 μm .

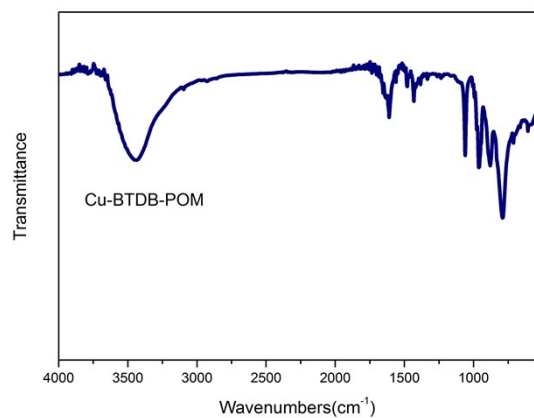


Figure S4 FT-IR spectrum of Cu-BTDB-POM.

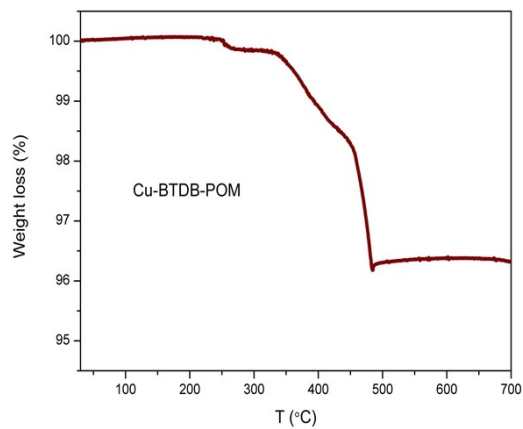


Figure S5 The TGA curve of Cu-BTDB-POM.

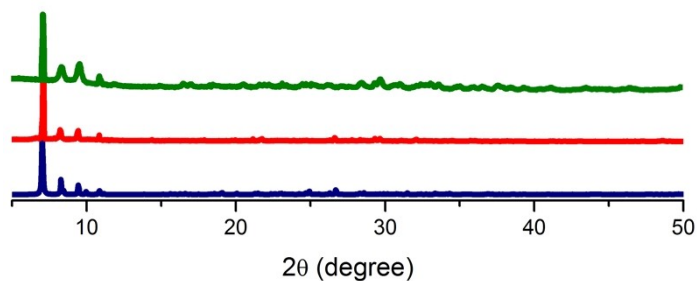


Figure S6 The simulated (blue) and experimental (red) PXRD patterns of Cu-BTDB-POM and PXRD patterns of Cu-BTDB-POM@CNT (green).

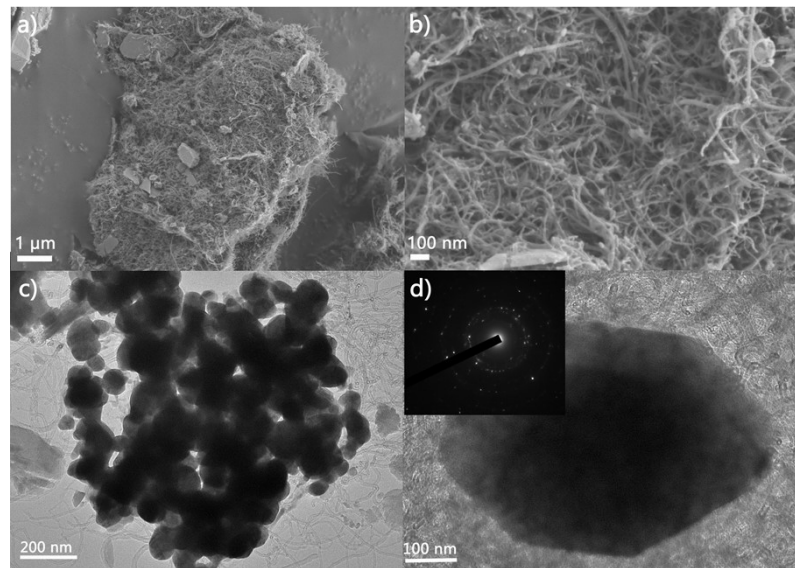


Figure S7 a), b) SEM images and c), d) TEM images of Cu-BTDB-POM@CNT.

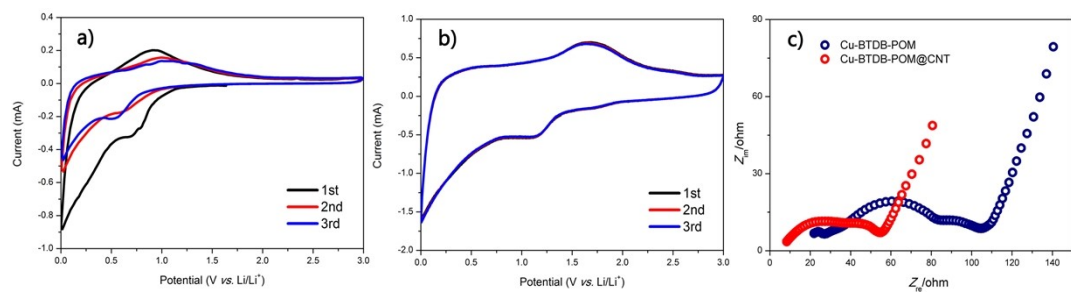


Figure S8 Cyclic voltammograms of Cu-BTDB-POM and Cu-BTDB-POM@CNT anodes at the range of 0.01-3.0 V (scan rate: 0.1 mV s⁻¹). Nyquist plots of Cu-BTDB-POM and Cu-BTDB-POM@CNT anodes after the first discharge-charge process.

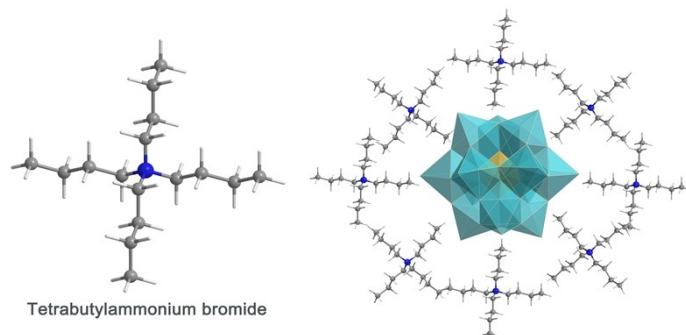


Figure S9 Schematic diagram of (NBu₄)₃[PMo₁₂O₄₀].

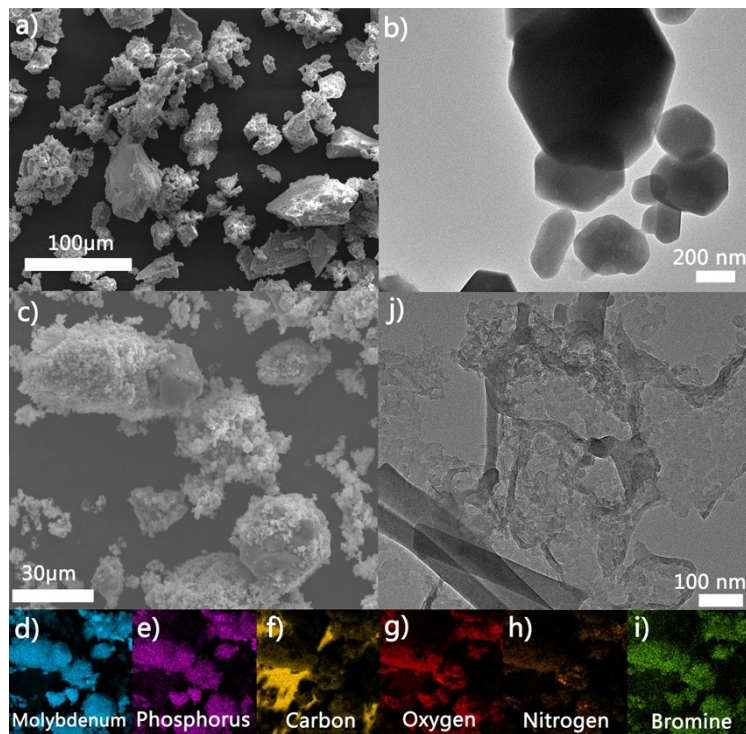


Figure S10 SEM images of a) $(\text{NBu}_4)_3[\text{PMo}_{12}\text{O}_{40}]$, c) $(\text{NBu}_4)_3[\text{PMo}_{12}\text{O}_{40}]@\text{PPy}@CNT$, elemental mapping of d)-i) $(\text{NBu}_4)_3[\text{PMo}_{12}\text{O}_{40}]@\text{PPy}@CNT$, and TEM images of j) $(\text{NBu}_4)_3[\text{PMo}_{12}\text{O}_{40}]@\text{PPy}@CNT$.

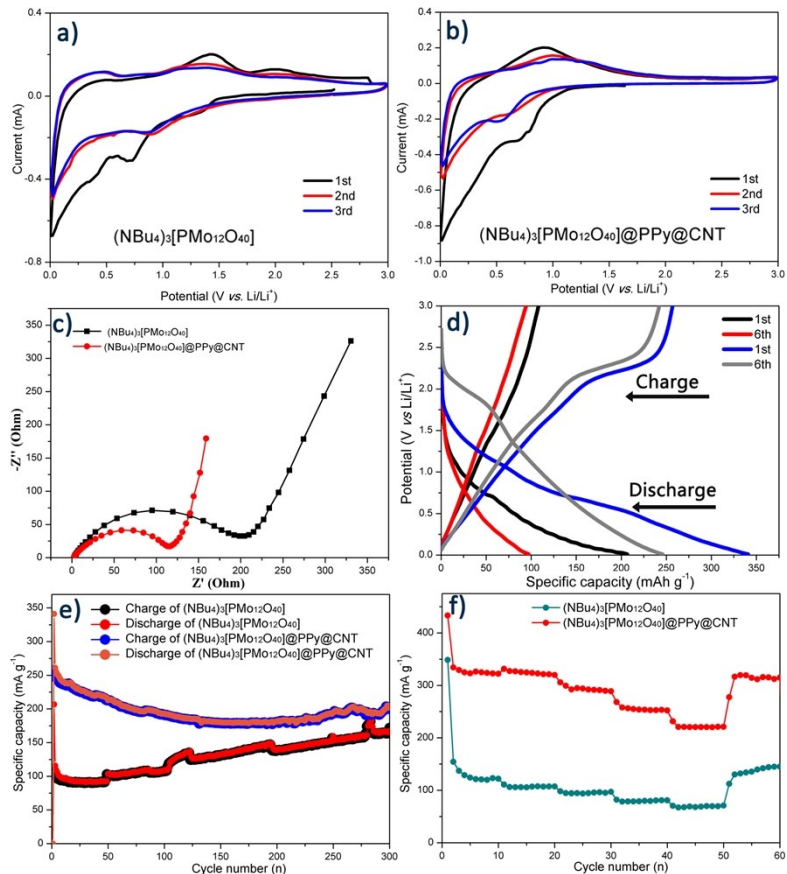


Figure S11 a)-c) CV and EIS of $(\text{NBu}_4)_3[\text{PMo}_{12}\text{O}_{40}]$ and $(\text{NBu}_4)_3[\text{PMo}_{12}\text{O}_{40}]@\text{PPy}@CNT$. d) The discharge/charge curves of $(\text{NBu}_4)_3[\text{PMo}_{12}\text{O}_{40}]$ and $(\text{NBu}_4)_3[\text{PMo}_{12}\text{O}_{40}]@\text{PPy}@CNT$. e) The discharge

capacities and the coulombic efficiencies of $(\text{NBu}_4)_3[\text{PMo}_{12}\text{O}_{40}]$ and $(\text{NBu}_4)_3[\text{PMo}_{12}\text{O}_{40}]@\text{PPy@CNT}$. f) Rate performances of $(\text{NBu}_4)_3[\text{PMo}_{12}\text{O}_{40}]$ and $(\text{NBu}_4)_3[\text{PMo}_{12}\text{O}_{40}]@\text{PPy@CNT}$ anodes at current densities of 100 mA g^{-1} to 2000 mA g^{-1} .

Table 1 Crystal data and structure refinement for Cu-BTDB-POM.

Compound reference	Cu-BTDB-POM
Chemical formula	$\text{C}_{24}\text{N}_{12}\text{H}_{13}\text{O}_{41}\text{PMo}_{12}\text{Cu}_2$
Formula Mass	2434.76
Crystal system	Triclinic
$a/\text{\AA}$	11.260(5)
$b/\text{\AA}$	11.656(5)
$c/\text{\AA}$	12.787(5)
$\alpha/^\circ$	79.302(5)
$\beta/^\circ$	84.606(5)
$\gamma/^\circ$	68.048(5)
Unit cell volume/ \AA^3	1529.0(11)
Temperature/K	293
Space group	<i>P-1</i>
No. of formula units per unit cell, Z	1
No. of reflections measured	5388
Final R_I values ($I > 2\sigma(I)$)	0.0808
Final $wR(F^2)$ values ($I > 2\sigma(I)$)	0.2390
Final R_I values (all data)	0.1461
Final $wR(F^2)$ values (all data)	0.2941
Goodness of fit on F^2	1.046
CCDC number	2121738

Table 2 Selected bonds lengths (\AA) and angles ($^\circ$) for Cu-BTDB-POM.

Mo(2)-O(20)	1.637(13)	Mo(3)-O(6)	1.918(15)
Mo(2)-O(19)	1.873(14)	Mo(3)-O(17)	1.926(15)
Mo(2)-O(5)	1.886(13)	Mo(3)-O(1)	2.33(2)
Mo(2)-O(23)	1.901(13)	Mo(3)-O(14)	2.518(19)
Mo(2)-O(4)	1.928(15)	Mo(4)-O(16)	1.644(15)
Mo(2)-O(11)	2.39(2)	Mo(4)-O(9)	1.862(13)
Mo(2)-O(14)	2.44(2)	Mo(4)-O(17)	1.872(14)

Mo(3)-O(22)	1.638(11)	Mo(4)-O(10)	1.920(13)
Mo(3)-O(23)	1.862(13)	Mo(4)-O(19)	1.933(13)
Mo(3)-O(7)	1.879(18)	Mo(4)-O(2)	2.41(2)
Mo(4)-O(14)	2.52(2)	Mo(1)-O(3)	1.872(16)
Mo(6)-O(18)	1.661(12)	Mo(1)-O(8)	1.880(17)
Mo(6)-O(12)	1.846(16)	Mo(1)-O(5)	1.897(15)
Mo(6)-O(4)	1.853(16)	Mo(1)-O(1)#1	2.36(2)
Mo(6)-O(9)#1	1.906(15)	Mo(1)-O(11)	2.47(2)
Mo(6)-O(3)	1.915(16)	Mo(5)-O(13)	1.670(14)
Mo(6)-O(2)#1	2.412(18)	Mo(5)-O(10)#1	1.832(15)
Mo(6)-O(11)	2.41(2)	Mo(5)-O(8)#1	1.896(17)
Mo(1)-O(21)	1.640(13)	Mo(5)-O(12)	1.898(16)
Mo(1)-O(6)#1	1.824(16)	Mo(5)-O(7)	1.920(18)
Mo(5)-O(2)#1	2.49(2)	O(1)-Mo(1)#1	2.36(2)
Cu(1)-O(18)	2.657(2)	O(2)-O(11)#1	1.79(3)
Cu(1)-N(1)	1.857(14)	O(2)-Mo(6)#1	2.412(18)
Cu(1)-N(2)	1.866(13)	O(2)-Mo(5)#1	2.49(2)
O(9)-Mo(6)#1	1.906(15)	O(8)-Mo(5)#1	1.896(17)
O(10)-Mo(5)#1	1.832(15)	O(6)-Mo(1)#1	1.824(16)
C(4)#3-C(5)-C(3)	117(2)	C(9)-C(10)-C(11)#2	118.3(18)
C(5)#3-C(4)-C(3)	118(2)	O(8)-Mo(1)-O(1)#1	65.8(8)
C(5)#3-C(4)-C(6)	120(2)	N(1)-Cu(1)-N(2)	174.0(7)
O(17)-Mo(4)-O(10)	154.4(8)	O(18)-Mo(6)-O(9)#1	100.2(8)
O(16)-Mo(4)-O(19)	100.4(8)	O(12)-Mo(6)-O(9)#1	87.3(7)
O(9)-Mo(4)-O(19)	156.5(8)	O(4)-Mo(6)-O(9)#1	158.3(7)
O(17)-Mo(4)-O(19)	87.5(6)	O(18)-Mo(6)-O(3)	99.3(9)
O(20)-Mo(2)-O(19)	102.5(8)	O(23)-Mo(3)-O(17)	87.3(6)
O(20)-Mo(2)-O(5)	100.3(8)	O(7)-Mo(3)-O(17)	157.0(8)
O(19)-Mo(2)-O(5)	90.8(6)	O(6)-Mo(3)-O(17)	87.8(7)
O(20)-Mo(2)-O(23)	103.4(8)	O(22)-Mo(3)-O(1)	159.0(8)

Symmetry transformations used to generate equivalent atoms: #1=-x+2,-y,-z+1; #2 -x+1,-y+1,-z+2; #3=-x+1,-y+2,-z.